

# ON THE EFFECTS OF THE ATMOSPHERIC CORRECTION OF THE GRACE MEASUREMENTS FOR STUDIES OF OCEANOGRAPHY

Lóránt FÖLDVÁRY<sup>1</sup> and Yoichi FUKUDA

Department of Geophysics  
Graduate School of Science  
Kyoto University  
Kitashirakawa Oiwake-cho  
Sakyo-ku, Kyoto 606-8502, Japan  
Phone/Fax +81-75-753-3912  
e-mail: fl@sci.fgt.bme.hu; fukuda@kugi.kyoto-u.ac.jp

Received: October 4, 2001

## Abstract

The forthcoming Gravity Recovery and Climate Experience (GRACE) gravity satellite will detect seasonal variations of the gravity field with very high accuracy. Seasonal variations of the mass redistribution would be useful data for several disciplines of geophysics and geodesy, if the seasonal mass variation could be unequivocally separated into its originating components. Seasonal mass variations are mainly provided by the atmosphere, oceans and hydrological processes. The main objective of this study is to analyze the effect of these fluids and/or the processes on the total gravity, focusing on the atmosphere, on the effect of atmospheric correction for studies of oceanography, in order to make use of the highly accurate measurements expected from the GRACE. The study found that a state-of-the-art marine geoid cannot be determined without considering the atmospheric mass redistribution, its effect on the ocean and the ocean's response to the atmospheric variation.

*Keywords:* GRACE, atmosphere, oceanic response.

## 1. Introduction

The basic idea of gravity satellites came from the inherent relationship between the gravitational forces and the orbital motion of a satellite. In general, the space missions launched in the past forty years have contributed to obtaining spatial variations of the Earth's gravity field. Recently, improvements in the accuracy of the measurements have allowed detection of the temporal variations in the gravity field. Investigations performed in the 1990's have considered variations of the gravity field over diurnal, inter-annual, decadal and secular terms [e.g. CHAO and AU, 1991; NEREM et al., 1993; CHAO and EANES, 1995; DONG et al., 1996].

---

<sup>1</sup>now MTA-BME Research Group for Physical Geodesy and Geodynamics, Department of Geodesy and Surveying, Budapest University of Technology and Economics, H-1521 Budapest, Hungary

In the case of a gravity satellite, its accuracy and resolution are strongly related to its altitude. Lower altitude allows for better spatial resolution, however, it involves larger atmospheric drag. The Laser Geodynamics Satellite (LAGEOS) missions 1 and 2 were the most profitable among the gravity satellites. Their altitude, 6000 km, was high enough to minimize atmospheric drag effects and low enough to provide good resolution. Recently, some relatively new techniques have become possible for use onboard satellites, promising a breakthrough in the resolution of the global gravity field. High-accuracy accelerometers make it possible to remove the non-gravitational accelerations from the total acceleration signal with fairly good reliability, therefore the altitude of the satellite can be radically reduced. By using GPS receivers, highly accurate orbit parameters can be continuously detected. The continuous precise detection of the altitude of the satellite allows for fewer orbital corrections to be needed; instead of correcting it by satellite manoeuvres, the altitude can itself be considered as a measured parameter. This results in long measurements, which allows for the determination of long periods variations as well. Both technologies will be applied on the GRACE, which is a gravity satellite mission under the supervision of the NASA and the GFZ (GeoForschungZentrum). The mission is scheduled to be launched in 2002 [further details in National Research Council (hereafter NRC), 1997].

The GRACE will be a low-low Satellite-to-Satellite tracking (SST) satellite performing range-rate measurements by radar interferometer [JEKELI, 1999]. The radar interferometry will be carried out on microwave frequencies. The inter-satellite range measurements will be done on two wavelengths, K-band (24 GHz) and Ka-band (32 GHz). The derivatives of the range will be obtained from the phase of the K-band signals. The payload of the mission also includes a high-accuracy GPS receiver for positioning, and a high-accuracy accelerometer for the detection of the non-gravitational acceleration. The GPS will continuously receive L1-band and L2-band signals. For further details see THOMAS [1999]. The GRACE will be on low altitude of about 450 km for long duration of time (nominal duration is five years). The orbits will be coplanar, circular and nearly polar. The separation distance of the satellites will vary between 100 and 400 km. The GRACE will determine a very accurate gravity field every 3 months. Frequency spectrum analyses show that the GRACE will perform its best in the longest wavelengths, between wavelength of 40000-800 km, equivalently up to a degree of 50 [VISSER, 1999]. The temporally varying geoid heights will be detected at scales of a few hundred kilometers and larger in a fine spatial resolution with an accuracy of some 0.1 mm [THOMAS, 1999; WAHR et al, 1998].

There is a wide range of temporal geophysical processes, which affects the gravity field. Large variations are caused by the solid earth processes, such as low-mantle convection, plumes, post-glacial rebound, earthquakes and volcanic activities. Beyond the solid earth, large temporal variations are also induced by the hydrospheric processes, such as ocean dynamics, water cycling, global sea-level rise, glaciologic processes and the atmospheric dynamics [NRC, 1997]. The spatial and the temporal scales of these processes differ from regional to global, and from diurnal to secular. The GRACE measurements will be useful for investigations

of seasonal, inter-annual geo-processes due to the global gravity field presentations every 3 months.

The temporal gravity field on the inter-annual and seasonal scale is induced by the ocean, the atmosphere and hydrological processes (surface and ground water, snow, ice). There are several applications of the temporal gravity field variations in the related disciplines [DICKEY et al., 1998]. It would be useful for oceanography to obtain more accurate ocean circulation models (OCM) by separating the steric and non-steric sea surface heights [NRC, 1997]. The determination of the deep ocean currents or consequently the sea-floor pressure variations would also improve the OCMs [DICKEY et al., 1999]. An accurate marine geoid would be useful for sea level rise investigations, for determination of ice mass changes of Antarctica and Greenland, etc. [WAHR et al., 2000]. Accurate detection of ground water variations would help develop studies of several hydrological processes [VAN DAM et al., 2001; RODELL et al., 1999]. A practical application of the improved hydrological signal would be its use for corrections of superconducting gravimetry [FUKUDA and FÖLDVÁRY, 2001; VAN DAM et al., 2001]. The detection of the seasonal gravity variations would improve the determination of the post-glacial rebounds and consequently, it would be useful for studying the viscosity of the underlying mantle [NRC, 1997].

One of the main goals expected from the GRACE is to detect seasonal oceanic variations. For some oceanographic applications of the GRACE measurements, first the atmosphere will be removed, i.e. for separating the steric and the non-steric heights. The aim of this study is to analyze the error effect of the atmospheric removal on the remaining hydrospheric signal. There have already been extensive studies performed concentrating on the hydrosphere. In the study of WAHR et al. [1998], a synthetic geoid was created, and subsequently, decomposed into oceanic and land water signals. The results show a recoverability of the geophysical processes up to a degree of about 40. The poor knowledge of the short-wavelength spherical harmonic coefficients was counteracted by using a Gaussian spatial function to emphasize the local (i.e. small-scale) features. This method yielded the detectability of seasonal hydrospheric mass variations at scales of a few hundred kilometers and larger to be within an order of magnitude of several millimeters of equivalent water thickness, or of 0.1 millibars.

## 2. Theoretical Background

### 2.1. Spherical Harmonic Coefficients of Temporal Gravity

If the density distribution of the Earth,  $\rho(r, \theta, \lambda)$ , is known, the spherical harmonic coefficients of the gravity field outside the Earth,  $C_{lm}$  and  $S_{lm}$ , can be written as

[e.g. HEISKANEN and MORITZ, 1967]

$$\begin{aligned} \begin{pmatrix} C_{l,m} \\ S_{l,m} \end{pmatrix} &= (2 - \delta_{0m}) \frac{(l-m)!}{(l+m)!} \frac{1}{Ma^l} \\ &\times \iiint_{\text{Earth}} \rho(r, \theta, \lambda) r^l P_{l,m}(\cos \theta) \begin{pmatrix} \cos m\lambda \\ \sin m\lambda \end{pmatrix} dV, \end{aligned} \quad (1)$$

where  $r$ ,  $\theta$ ,  $\lambda$  are the spherical coordinates (radial distance, colatitude and east longitude, respectively),  $\delta_{0m}$  is the Cronecker delta,  $M$  is the mass and  $a$  is the semi-major axis of the Earth,  $P_{l,m}$  is the associated Legendre polynomial of degree  $l$  and order  $m$ . The integration is performed over the entire volume of the Earth,  $V$ , including its fluid envelope (hydrosphere and atmosphere).

The applied form of (1) in this study differs a little bit (2), since it considers the temporal variations. Thus the surface density and the corresponding spherical harmonic coefficients are replaced by their temporal variations, i.e.  $\Delta\rho(\theta, \lambda, t)$ ,  $\Delta C_{l,m}(t)$  and  $\Delta S_{l,m}(t)$ , respectively. The solid Earth tides were modelled in the terms of the Earth's load Love numbers,  $k'_l$  [FARELL, 1972], and added to Eq. (1) (see section 4).

The semi-major axis of the Earth,  $a$ , was approximated with an average radius of the Earth,  $R$ . Let us assume a radially homogeneous density field,  $\rho_s(\theta, \lambda)$ . Then the spatial mass element,  $\rho(r, \theta, \lambda) dV$  can be written in spherical coordinates as  $R^2 \rho_s(\theta, \lambda) d\sigma$ . Substituting the average density of the Earth as  $\rho_{ave} = M/V_{\text{Earth}}$ , where the volume of the Earth is  $V_{\text{Earth}} = 4R^3\pi/3$  normalizing the coefficients,  $\Delta\bar{C}_{l,m}(t)$  and  $\Delta\bar{S}_{l,m}(t)$ , Eq. (1) becomes

$$\begin{aligned} \begin{pmatrix} \Delta\bar{C}_{l,m}(t) \\ \Delta\bar{S}_{l,m}(t) \end{pmatrix} &= \frac{4\pi}{3} \frac{1+k'_l}{2l+1} \frac{1}{R\rho_{ave}} \\ &\times \iint_{\text{Earth}} \Delta\rho(\theta, \lambda, t) P_{l,m}(\cos \theta) \begin{pmatrix} \cos m\lambda \\ \sin m\lambda \end{pmatrix} d\sigma. \end{aligned} \quad (2)$$

The integration was carried out over a unit sphere with a surface element  $\Delta\sigma$  ( $d\theta$ ,  $d\lambda$ ).

## 2.2. Degree Variances and the Degree Geoid Height Anomaly Spectrum

From normalized Stokes coefficients of the seasonal gravity,  $\Delta\bar{C}_{l,m}(t)$  and  $\Delta\bar{S}_{l,m}(t)$ , degree variance values,  $\sigma_l^2$ , were derived as [HEISKANEN and MORITZ, 1967]

$$\sigma_l^2 = \sum_{m=0}^l \left( \Delta\bar{C}_{l,m}^2 + \Delta\bar{S}_{l,m}^2 \right). \quad (3)$$

Since the degree variance is a dimensionless quantity, which is proportional to the degree spectra of the gravity field variations, it is desirable to represent it as a gravity

related quantity. Using the method of NRC [1997] degree variance spectra in this study are shown as degree variance of expected geoid height anomalies, which are derived as  $\sigma_N = a\sigma_l$ , where  $a$  could be the semi-major axis of the Earth, or an average value of the Earth's radius. The graph of  $\sigma_N$  is called the degree geoid height anomaly spectrum.

### 3. Data and Data-Preprocessing

The National Centers for Environmental Prediction/National Center for Atmospheric Research (NCEP/NCAR) Reanalysis Project produced a global analysis of the atmospheric field over 40 years and was completed in 1997 [details in KALNAY et al., 1996]. The data produced by this analysis were employed for atmospheric pressure, soil moisture and snow depth in this present study.

The sea surface height data were the latest version (4B) of the Parallel Ocean Climate Model (POCM). These data consist of sea surface height values for approximately every ten days. The POCM estimates the variations of the sea-floor pressure in the ocean. These data cover the oceanic areas from 65°N to 75°S in latitude. The acquired data had already been processed by SATO et al. [2000]. The previous processing of the data included the thermal steric correction.

Unfortunately, only about three years of the sea surface height variation data set were available between October 1992 and December 1995. The 3.25 years of data, however, involve detectable temporal variations up to the annual term.

## 4. Modelling of Seasonal Mass Variations

### 4.1. Modelling of the Atmosphere

The mass variation of a column of atmosphere over a surface element of the Earth was considered as a condensed mass at the surface element. Let the temporal variation of the atmospheric pressure be denoted by  $\Delta P(\theta, \lambda, t)$ . Then,

$$\Delta\rho(\theta, \lambda, t) = \frac{\Delta P(\theta, \lambda, t)}{g}, \quad (4)$$

where  $\Delta\rho(\theta, \lambda, t)$  is the surface density variation and  $g$  is the gravitational acceleration.

#### 4.1.1. Oceanic Response to Atmospheric Mass Variations; IB and NIB

Geophysical fluids considerably influence each other's dynamics. Variations in the atmospheric pressure deform the oceanic surface, i.e. the oceanic mass, which re-deforms the atmosphere, resulting in secondary atmospheric mass variation. The

secondary variation of the atmospheric mass induces significant variations compared to the global atmospheric mass variations [FÖLDVÁRY and FUKUDA, 2001/1]. Since the primary and the secondary atmospheric mass variations occur on similar wavelengths of mass variation, it is impossible to distinguish them by any kind of measurement, thus the secondary variations could be treated as an error of the primary variations. Since the atmosphere has a strong seasonal variation, the most significant uncertainties are also expected to occur on this frequency, limiting the applicable accuracy of a marine geoid.

Two theoretical extremes of the mutual dynamics of the atmosphere and the ocean are considered in geophysics, the IB (inverted barometer) and the NIB (non-inverted barometer). The IB model assumes that to the change in atmospheric pressure, the underlying ocean immediately reacts by flows, and totally dissipates it. The NIB assumes that the atmospheric mass redistribution over the ocean remains local. There are no reactions by flows, and pressure changes are conducted down to the bottom of the ocean.

In reality, the oceanic response lies between the IB and the NIB cases. For shorter variation, such as the diurnal term, the NIB is maybe reasonable, because of the slowness of the current flow for the time frame. However, for the secular term, the IB is a much more realistic model, because of the quickness of current flow for the secular time frame. The real question is how the seasonal time frame variations perform. It validates any kind of, even unrealistic, intermediate concept.

Models have been computed for these two basic cases, and there have also been attempts to create intermediate models between them. These intermediate models were performed by spatially combining the IB and NIB responses over the globe.

#### *4.1.2. Shallow Water*

The dynamics of geophysical fluids in shallow water areas is a well-analyzed issue in geophysics [e.g. PEDLOSKY, 1979]. Around the coastal area, there is not enough depth to dissipate any pressure disturbance by flows. Most of the pressure signal reaches the bottom of the ocean. Therefore, in shallow water, the NIB is more preferable to IB. There is no clear depth to divide the shallow and the deep waters. In this study two values of depth, 500 m and 2000 m, were tested.

#### *4.1.3. Spatial Separation*

The topographic features of the Earth's crust, i.e. continents, seamounts, ridges, trenches, rifts and swells divide the world ocean into smaller reservoirs. Even though most of these reservoirs are not absolutely isolated from each other, and the water can change place between them, the separating effect of the topography can be essential and added to this study. Since the degree of the separating effect

differs feature by feature, the spatial function and the resolution of the effective separation is difficult to model. E. g. seamounts primarily affect the deep ocean currents and only indirectly affect the sea surface variations; their effect on the atmosphere-ocean mutual dynamics is unknown.

The world ocean in this study was divided into four smaller reservoirs/basins: Indian Ocean, Atlantic Ocean, Pacific Ocean and Arctic Ocean, where no connection between the basins was assumed. For this model, the shallow water theory (see 4.2.2.) was also applied. Again, two values of depth, 500 m and 2000 m, were tested, which values indicate (1) the depth of the allowed marine topography, and (2) the depth of the assumed shallow water effect as well.

#### 4.2. Modelling of the Ocean

When modelling the ocean, it was again assumed that the total volumetric mass change of the ocean over a surface element was condensed to be the bottom of the ocean, eliminating the depth factor.

$$\Delta\rho(\theta, \lambda, t) = \Delta H(\theta, \lambda, t) \rho_{\text{water}}, \quad (5)$$

where  $\Delta\rho(\theta, \lambda, t)$  is the surface density variation,  $\Delta H(\theta, \lambda, t)$  is the non-steric sea surface height variation, and  $\rho_{\text{water}}$  is the density of the water.

#### 4.3. Modelling of the Land Water

The term ‘land water’ in this study is used for denoting the global continental water storage. Since, in a spatial sense, the water-level variation of the rivers is negligible, the modelled seasonal land water mass variation constrained on the ground water (via soil moisture) and the snow mass. The assumption for the soil moisture was uniform depth of ground water,  $h_{sm} = 65$  cm, with uniform density,  $\rho_{\text{water}} = 1000$  g/cm<sup>3</sup>. For the case of snow, its density was assumed to be uniform with a value of  $\rho_{\text{snow}} = 300$  g/cm<sup>3</sup>.

$$\Delta\rho(\theta, \lambda, t) = \Delta c_{sm}(\theta, \lambda, t) h_{sm} \rho_{\text{water}} + \Delta h_{\text{snow}}(\theta, \lambda, t) \rho_{\text{snow}}, \quad (6)$$

where  $\Delta\rho(\theta, \lambda, t)$  is the surface density variation,  $\Delta h_{\text{snow}}(\theta, \lambda, t)$  and  $\Delta c_{sm}(\theta, \lambda, t)$  are the variations of the snow thickness and of the soil moisture capacity, respectively.

### 5. Modelling of the GRACE Errors

The GRACE modelling followed the methodology of JEKELI and RAPP [1980]. It considers the accuracy of a low-low SST configuration from the accuracy of

the range-rate measurements between the two satellites,  $m(v)$ , and the geometrical parameters of the satellites. The weak point of this technique is that it assumes the spatial density of the measurements to be uniform. This uniform spatial resolution,  $\Delta\sigma$ , is defined as [JEKELI and RAPP, 1980]

$$\Delta\sigma = 2\pi^2 \frac{S}{D}, \quad (7)$$

where  $D$  is the nominal duration of the mission, and  $s$  is the measurement sampling interval.

Let  $R$  denote the radius of the Earth,  $h$  the altitude of the satellite,  $k$  the gravitational constant and  $M$  the mass of the Earth, then  $r = R+h$ , and  $\gamma = kM/R^2$ . The degree variance of the satellite measurements in terms of geoid heights,  $m(N)$ , is [JEKELI and RAPP, 1980]

$$m(N)_l = \frac{R}{\sqrt{\gamma r}} \sqrt{\frac{\Delta\sigma}{4\pi}} m(v) \left[ \sum_{n=2}^l \frac{\beta_n^2 (2n+1)}{2(1-P_n(\cos \psi_{PQ}))} \left(\frac{r^2}{R^2}\right)^{n+1} \right]^{\frac{1}{2}}, \quad (8)$$

where  $N$  indicates the geoid heights, and  $v$  the range-rate.  $l$  is the degree, and  $\beta_n$  is a coefficient that can be approximated by the Sjoberg recursive formula [SJOBERG, 1980].  $P_n$  is the Legendre polynomial, where the angle of  $\psi_{PQ}$  indicates the separation angle between the two satellites.

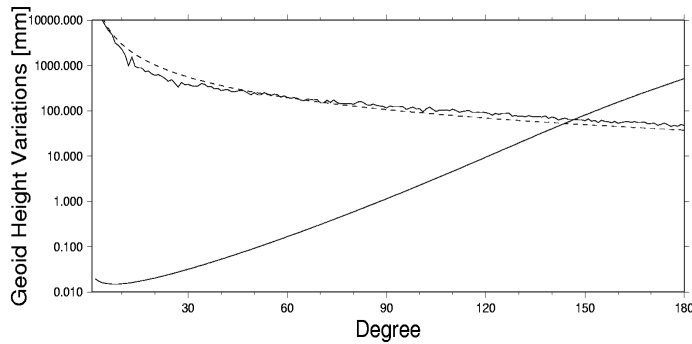


*Fig. 1.* The sensitivity of the GRACE characterized by geoid height anomalies, as the function of the degree  $l$ . The dashed line indicates Kaula's rule of thumb, along with the EGM96 errors (solid line).

The expected degree variance of the range-rate measurements of the GRACE is assumed to follow a white noise spectrum, with a PSD (power spectral density) of  $0.5\mu\text{m/s}/\sqrt{\text{Hz}}$  [THOMAS, 1999]. The orbit of the satellites was modelled to be coplanar, polar and circular. The modelled geometrical parameters were the altitude,  $h = 400$  km, separation distance between the two satellites,  $S = 300$  km, sampling

interval,  $s = 10$  s, duration,  $D = 3$  months. This yielded a  $\Delta\sigma = 300$  square minutes of arc uniform spatial resolution. The degree spectrum of the sensitivity of the GRACE is shown in *Fig. 1*, along with Kaula's rule of thumb [KAULA, 1966].

## 6. Modelling of an Artificial GRACE Measurement Signal

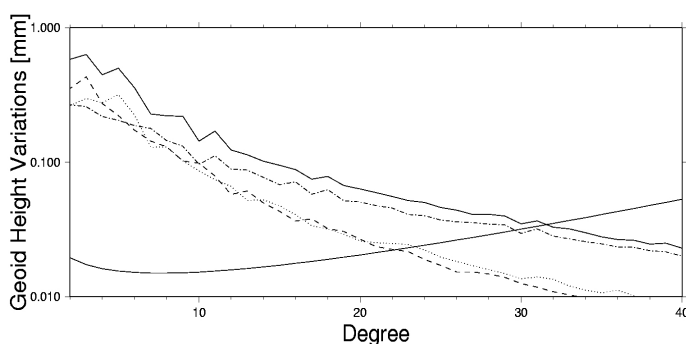


*Fig. 2.* Geoid height anomalies of seasonal geophysical fluids compared with the sensitivity of the GRACE mission, as function of the degree  $l$ . The dashed line indicates the effect of the atmosphere (IB) on the seasonal geoid, the dotted line is that of the land water (soil moisture + snow pack), the dashed-dotted line is that of the ocean, and the solid line is the composed seasonal geoid signal (atmosphere + ocean + land water).

The GRACE measurement signal was modelled by simply adding up the atmospheric, the hydrologic and the ocean geoid height variation models [FÖLDVÁRY and FUKUDA, 2001/2]. The degree geoid height anomaly spectrum of the seasonal composed signals is shown in *Fig. 2* along its contributors.

Because of the different source of the data for land water and ocean, the total mass of water was not constant in time. Thus first it was necessary to conserve it, resulting in an artificial hydrosphere model [FÖLDVÁRY and FUKUDA, 2001/2].

At this point, the different models for oceanic response to atmospheric pressure (see 4.1.) have been neglected. An IB reaction was assumed, and the possible differences were analyzed later.

In the study of WAHR et al [1998], the degree anomaly spectra show a detectability of the seasonal geoid height variations up to about degree 40 (see Figure 1a for the annual term). In this study it was up to about 25–30 (see *Fig. 2* here for all terms). This difference derived from the assumed error variance of the GRACE rather than from the modelled geophysical fluids. The difference in the error variance of the GRACE could be derived from different parameterization of

the geometrical configuration. Slight differences of geometrical parameterization should yield notably large differences in the degree geoid height anomaly spectrum. Unfortunately, some applied geometrical parameters were not detailed in WAHR et al [1998].

## 7. Atmospheric Correction

For separating the steric and the non-steric heights from combined GRACE and satellite altimeter measurements, the atmospheric mass would be corrected from the total gravity signal. In practice, for this case, the removed atmosphere is assumed to be IB. In this recent study this assumption is thought to be too rough; the accuracy of the GRACE is assumed to be sensitive for the errors of an inaccurate atmospheric correction. The atmospheric correction was modelled for the basic atmospheric models, i.e. IB and NIB (see 4.1.1), and the intermediate models (see 4.1.2 and 4.1.3).

An atmosphere-corrected model is a good approximation for the recovered hydrosphere-induced gravity field (hereafter ‘atmosphere-removed’ gravity is equivalent with the ‘recovered hydrosphere-induced’ gravity). Since during the modelling of the GRACE measurements the IB-atmosphere was assumed, at this point, the IB-removal describes an idealistic, perfect atmosphere-corrected, hydrosphere-only-induced gravity. For all the other cases, NIB and intermediate atmospheres, an atmospheric correction error is assumed to worsen the recoverability of the hydrosphere. The different models describe different rates of the role of the atmospheric correction error.

Similarly to the degree geoid height anomaly spectra in *Fig. 1*, that of the atmosphere removed models were computed by (3). These models describe several models for the ‘recovered’ hydrospheric gravity. Therefore, their differences with the ‘real’ hydrospheric gravity describe the atmospheric correction errors, and are shown in *Fig. 3*.

The comparing of these differences with the expected resolution of the GRACE shows that different assumptions for the atmosphere have visible effects by the GRACE in the first 10 degrees. Since the modelled accuracy of the GRACE was found to be poorer in this study than in others [VISSER, 1999; WAHR et al., 1998], the role of the atmospheric correction error can even be more emphasized.

The same feature was analyzed by correlating the geoid height variations of the modelled ‘real’ and ‘recovered’ hydrospheres. For the correlation computation the geoid height variations were assumed to be both temporally and spatially independent. Practically, the ‘recover’ hydrosphere geoids were expanded into time series of geoid height variations in every grid, and then correlated to that of the ‘real’ hydrosphere grid by grid. Finally, the resulting correlation fields were spatially averaged into correlation values, and these are shown in *Table 1*.

The *Table 1* shows the effect of the atmospheric correction error. The correlations were computed between the models of the ‘recovered’ (atmosphere corrected)

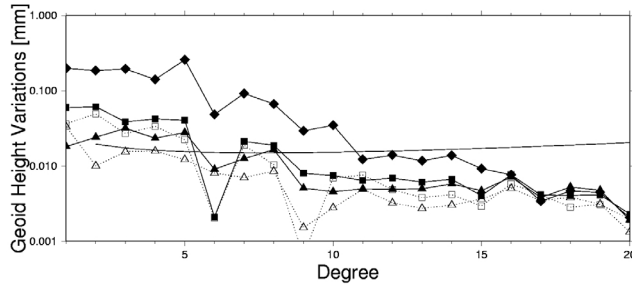


Fig. 3. Differences of geoid height anomalies of atmosphere-removed and hydrospheric models, as a function of the spherical harmonic degree 1. The largest signal produced by the NIB-removed minus hydrosphere case (filled diamond). Similarly the hydrosphere was also subtracted from the intermediate atmosphere removed models. These are indicated with squares for the basin models (filled – 2000, blank – 500) and with triangles for the shallow water models (filled – 2000, blank – 500).

Table 1. The correlations describe the effect of the atmospheric correction. The correlation values compared were the atmosphere removed models with the hydrosphere (1<sup>st</sup> column), the atmosphere removed model over the oceanic region with the ocean (2<sup>nd</sup> column), and the atmosphere removed model over the land region compared with the land water (3<sup>rd</sup> column).

	Atmosphere removed vs. hydrosphere	Atmosphere removed vs. ocean (over the ocean)	Atmosphere removed vs. land water (over the land)
IB	1.000	0.930	0.952
Shallow water (500)	0.981	0.913	0.942
Shallow water (2000)	0.956	0.879	0.930
Basin separation (500)	0.958	0.893	0.919
Basin separation (2000)	0.936	0.862	0.910
NIB	0.626	0.380	0.869

and the ‘real’ hydrospheres. The table also shows the ‘recovered’ signal over the oceanic region compared with the ‘real’ ocean signal (2<sup>nd</sup> column), and similarly, with that over the land region (3<sup>rd</sup> column).

Differences in the correlation values of the first column of the table result from the differences of the removed atmospheric model. Since the assumed atmosphere during the composition was IB, the IB removal results are in total agreement. The principally different NIB removal yields a weak correlation. All the intermediate models give a correlation of at least 0.936. These results are according to the

expectations. If reality is similar to the NIB, then the atmospheric removal, with an assumed IB or intermediate model, would be considerably erroneous. However, for the few-week time frames, i.e. GRACE data presentations, there are reasonably expectable some degrees of IB response to exist at least at the very central basins of the oceans. Since the most probable places of an IB response are the deep oceans, which yield a significantly large area of the Earth, by assuming any degree of IB response, it implies a large room of IB, this is practically always larger than the area of NIB. This feature was obvious in the fact that all attempts of defining an intermediate model yielded a more IB-type response than a NIB-type one (see *Table 1*). The long and short of it, that involves a high similarity with the IB, and a very low similarity with the NIB by assuming existence of an IB response on any small degree. Therefore the theoretical validity of the maximal error (i.e. NIB) is very low.

The GRACE recovery would provide useful measurements for oceanography. Thus, the accurate differentiation of the land-water and the ocean induced gravity variations are of importance. The land water-/ocean-induced geoids are assumed to be approximated by the atmosphere corrected geoid over the land/ocean, i.e. the 3<sup>rd</sup> and the 2<sup>nd</sup> columns of *Table 1*. These models are sufficient approximations for areas far from the coasts. However, at the coastlines, the gravity effect of both the land water and the ocean is significant, e. g. the mass of the near-coast land water affects significantly the nearby marine geoid, and vice versa. In addition, the applied atmospheric correction (IB) at the coastlines induces a further error, since an NIB reaction is more reliable that is due to the lack of enough room of compensation, i.e. shallow water effect.

## 8. Discussion and Summary

The observations of the GRACE will involve the integration of all the effects of mass redistributions. Hence gravity signals from known redistribution sources need to be carefully removed for the purposes of studies involving other, unknown, mass redistribution sources. For the present study it is assumed that certain geophysical phenomena are known better than those being sought. This knowledge of their characteristics; amplitude, frequency and phase for cyclic terms, and trend for secular changes, can be used to eliminate their effects from the integrated gravity signals. Even though in several regions, i.e. in the Southern ocean, or over Antarctica, the atmospheric surface pressure field is known to be quite inadequate, it is still one of the best-measured quantities compared to other surface mass redistributions. Therefore, for several applications of the GRACE measurements, the elimination of the atmosphere will be desired.

WAHR et al. (1998) found that, the elimination of the atmospheric mass from satellite gravity measurements has no practical significance. For several oceanographic applications in their section 5.1, this can be accepted, however, their case 3, that is the combination of GRACE and altimeter measurements for separating

the steric and non-steric heights, we argue against their reasoning. WAHR et al. (1998) conclude that (1) ‘altimeter data records include (...) estimated corrections for the ocean’s response to pressure’ and (2) the ‘GRACE results will most likely be provided (...) with the combined effects of atmospheric pressure and the ocean’s response to pressure already removed’. At this point we believe that the provided data will contain atmospheric error to a certain, probably large extent, which makes the data inappropriate for the purpose. Thus for steric/non-steric analyses an improved method for eliminating the atmosphere from the raw data of both measurements would only be acceptable.

Following this concept, in this study first a seasonal gravity signal was created, subsequently the error effect of the atmospheric elimination was analyzed due to the inaccuracies of the oceanic response to atmospheric variations.

Since both NIB and IB are theoretical extremes, semi-realistic intermediate models were created in this study. It is important to reiterate that, during the composition an extreme case (IB) was assumed, therefore the differences with the other extreme case (NIB) are an over-estimation; it should be much smaller by assuming an intermediate case. Recently due to lack of information, it is impossible to prefer any of the intermediate models. However, the inexactness of an intermediate model definition yields much smaller errors than using any of the extreme cases (see *Fig.3* and *Table 1*).

The applied mathematics of this study, i.e. spherical harmonics, degree spectrum, are valid for modelling global variations. However, it cannot reflect the spatial variation of the problem. The atmospheric correction errors are reasonably constraining on the coastal areas. The analysis performed in this study found the atmospheric uncertainties having a visible effect on the global signal, therefore, for local scales applications, the atmospheric correction errors are believed to be notably large along the coast lines.

## References

- [1] CHAO, B. F. – AU, A. Y., Temporal Variations of the Earth’s Low-degree Zonal Gravitational Field Caused by Atmospheric Mass Redistribution: 1980–1988, *Journal of Geophysical Research*, **96** No. B4 (1991), pp. 6569–6575.
- [2] CHAO, B. F. – EANES, R., Global Gravitational Changes due to Atmospheric Mass Redistribution as Observed by the Lageos Nodal Residuals, *Geophysical Journal International*, **122** (1995), pp. 755–764.
- [3] DICKEY, J. O. – BENTLEY, C. R. – BILHAM, R. – CARTON, J. A. – EANES, R. J. – HERRING, T. A. – KAULA, W. M. – LAGERLOEF, G. S. E. – ROJSTACZER, S. – SMITH, W. H. F. – VAN DEN DOOL, H. M. – WAHR, J. W. – ZUBER, M. T., Satellite Gravity: Insights into the Solid Earth and its Fluid Envelope, *Eos, Trans. AGU*, **79** (20) (1998), pp. 237–241.
- [4] DICKEY, J. O. – BENTLEY, C. R. – BILHAM, R. – CARTON, J. A. – EANES, R. J. – HERRING, T. A. – KAULA, W. M. – LAGERLOEF, G. S. E. – ROJSTACZER, S. – SMITH, W. H. F. – VAN DEN DOOL, H. M. – WAHR, J. W. – ZUBER, M. T., Gravity and the Hydrosphere: New Frontier, *Hydrological Science-Journal-des Sciences Hydrologiques*, **44** (3) (1999).
- [5] DONG, D. – GROSS, R. S. – DICKEY, J. O., Seasonal Variations of the Earth’s Gravitational Field: an Analysis of Atmospheric Pressure, Ocean Tidal, and Surface Water Excitation, *Geophysical Research Letters*, **23** (1996), pp. 725–728.

- [6] FARELL, W. E., Deformation of the Earth by Surface Loads, *Reviews of Geophysics and Space Physics*, **10** (1972), pp. 761–797.
- [7] FÖLDVÁRY, L. – FUKUDA, Y., IB and NIB Hypotheses and their Possible Differentiation by GRACE, *Geophysical Research Letters*, **28** No. 4 (2001/1) pp. 663–666.
- [8] FÖLDVÁRY, L. – FUKUDA, Y., Evaluation of Temporal Variations on the Gravity Field Caused by Geophysical Fluids and their Possible Detection by GRACE, *Proceedings of IAG International Symposium GGG2000*, Banff, Alberta, Canada, in press, 2001/2.
- [9] FUKUDA, Y. – FÖLDVÁRY, L., Environmental Correction for the Precise Gravity Observations by Mean of Satellite Gravity Data, *Journal of Geodetic Society of Japan*, **7** No. 2 (2001), pp. 679–685.
- [10] HEISKANEN, W. A. – MORITZ, H., *Physical Geodesy*, W. H. Freeman and Company, San Francisco and London, pp. 364, 1967.
- [11] JEKELI, C. – RAPP, R. H., Accuracy of the Determination of Mean Anomalies and Mean Geoid Undulations from a Satellite Gravity Mapping Mission, *Report No. 307*, Department of Geodetic Science, The Ohio State University, Columbus, 1980.
- [12] JEKELI, C., The Determination of Gravitational Potential Differences from Satellite-to-Satellite Tracking, *Celestial Mechanics and Dynamical Astronomy*, **75** (1999), pp. 85–101.
- [13] KALNAY, E. – KANAMITSU, N. – KISTLER, R. – COLLINS, W. – DEAVEN, D. – GANDIN, L. – IREDELL, M. – SAHA, S. – WHITE, G. – WOOLLEN, J. – ZHU, Y. – CHELLIAH, M. – EBISUZAKI, W. – HIGGINS, W. – JANOWIAK, J. – MO, K. C. – ROPELEWSKI, C. – WANG, J. – LEETMAA, A. – REYNOLDS, R. – JENNE, R. – JOSEPH, D., The NCEP/NCAR 40-Year Reanalysis Project, *Bulletin of the American Meteorological Society*, **77** No. 3 (1996), pp. 437–471.
- [14] KAULA, W. M., *Theory of Satellite Geodesy*, Blaisdell Publishing Company, Waltham, Massachusetts, Toronto and London, pp. 128, 1966.
- [15] National Research Council (NRC): Satellite Gravity and the Geosphere, National Research Council Report, pp. 112, National Academy Press, Washington, D. C., 1997.
- [16] NEREM, R. S. – CHAO, B. F. – AU, A. Y. – CHAN, J. C. – KLOSKO, S. M. – PAVLIS, N. K. – WILLIAMSON, R. G., Temporal Variations of the Earth's Gravitational Field from Satellite Laser Ranging to Lageos, *Geophysical Research Letters*, **20** (1993), pp. 595–598.
- [17] PEDLOSKY, J., *Geophysical Fluid Dynamics*, Springer-Verlag, New York, pp. 626, 1979.
- [18] RODELL, M. – FAMIGLIETTI, J. S., Detectability of Variations in Continental Water Storage from Satellite Observations of the Time Dependent Gravity Field, *Water Resources Research*, **35** No. 9 (1999), pp. 2705–2723.
- [19] SATO, T. – FUKUDA, Y. – AOYAMA, Y. – MCQUEEN, H. – SHIBUYA, K. – TAMURA, Y. – ASARI, K. – OOE, M., On the Observed Annual Gravity Variation and the Effect of Sea Surface Height Variations, submitted to *Physics of the Earth and Planetary Interiors*, 2000.
- [20] SJOBERG, L., A Recurrence Relation for the  $\beta_n$ -Function, *Bulletin Geodesique*, **54** No. 1 (1980), pp. 69–72.
- [21] THOMAS, J. B., An Analysis of Gravity-Field Estimation Based on Intersatellite Dual-1-Way Biased Ranging, *JPL Publication*, 98–15, 1999.
- [22] VAN DAM, T. M. – WAHR, J. – CHAO, Y. – LEULIETTE, E., Predictions of Crustal Deformations and of Geoid and Sea-Level Variability Caused by Oceanic and Atmospheric Loading, *Geophysical Journal International*, **129** (1997), pp. 507–517.
- [23] VAN DAM, T. M. – WAHR, J. – MILLY, P. C. D. – FRANCIS, O., Gravity Changes Due to Continental Water Storage, *Journal of Geodetic Society of Japan*, in press, 2001.
- [24] VISSER, P. N. A. M., Gravity Field Determination with GOCE and GRACE, *Advanced Space Research*, **23** No. 4 (1999), pp. 771–776.
- [25] WAHR, J. S. – MOLENAAR, M. – BRYAN, F., Time Variability of the Earth's Gravity Field: Hydrological and Oceanic Effects and their Possible Detection Using GRACE, *Journal of Geophysical Research*, **103** No. B12 (1998), pp. 30205–30229.
- [26] WAHR, J. S. – WINGHAM, D. – BENTLEY, C., A Method of Combining ICESat and GRACE Satellite Data to Constrain Antarctic Mass Balance, *Journal of Geophysical Research*, **105** No. B7 (2000), pp. 16279–16294.